



## Influence of free ferrite on the mechanical properties of high strength intercritical Austempered Ductile Iron

A. D. Basso, M. Caldera, N. E. Tenaglia, D. O. Fernandino, R. E. Boeri

INTEMA4, Universidad Nacional de Mar del Plata-CONICET, Av. Colón 10850, Mar del Plata, B7606BVZ, Argentina

abasso@fimdp.edu.ar, <https://orcid.org/0000-0002-6167-4426>

mcaldera@fimdp.edu.ar, <https://orcid.org/0000-0002-8677-540X>

dfernandino@fimdp.edu.ar, <https://orcid.org/0000-0003-4647-2663>

ntenaglia@fimdp.edu.ar, <https://orcid.org/0000-0001-6372-8881>

boeri@fimdp.edu.ar, <https://orcid.org/0000-0001-7083-579X>



**Citation:** Basso, A. D., Caldera, M., Tenaglia, N. E., Fernandino, D. O., Boeri, R. E., Influence of Free Ferrite on the Mechanical Properties of High Strength Intercritical Austempered Ductile Iron, *Frattura ed Integrità Strutturale*, 61 (2022) 519-529.

**Received:** 28.05.2022

**Accepted:** 09.06.2022

**Online first:** 19.06.2022

**Published:** 01.07.2022

**Copyright:** © 2022 This is an open access article under the terms of the CC-BY 4.0, which permits unrestricted use, distribution, and reproduction in any medium, provided the original author and source are credited.

**ABSTRACT.** The first stage of this study investigates the precipitation of free ferrite from the austenite on fully austenitized ductile iron. Several sets of samples of low alloy ductile iron are fully austenitized and then cooled down to different temperatures and different times within the intercritical austenite-ferrite-graphite phase field.

Based on these results, heat treatment cycles aimed at obtaining microstructures composed of free ferrite and ausferrite are carried out. Tensile, impact and toughness tests are performed to characterize the mechanical properties. The results show that, related to the high strength austempered ductile iron grades, the best combinations of properties were obtained from the mixed structures composed of 5% free ferrite and 95% ausferrite, resulting from the austempering at 280°C. These amounts of free ferrite allow obtaining an increase of the elongation (about 50%) and impact toughness (about 10%) while the tensile strength and fracture toughness decrease by about 1.5 and 15% respectively.

**KEYWORDS.** Ductile Iron; Free ferrite; Mechanical properties; Heat treatments.

## INTRODUCTION

The continuous need for the development of ductile irons (DI) of improved mechanical properties has led the researchers to investigate the usefulness of the development of complex microstructures. The applicability of metallic matrices formed by free ferrite and ausferrite obtained through the austempering of partially austenitized ductile irons, a material usually called 'IADI' (Intercritically Austempered Ductile Iron), has received some attention [1-13]. Specific thermal cycles have been developed in order to obtain IADI microstructures. The first paper concerning this subject matter was written by Aranzabal et al. [1]. The authors obtained different variants of IADI by modifying the silicon level of



the melts and heat-treating ferritic DI at different austenitizing temperatures. During the austenitizing stage, different amounts of austenite nucleate and grow as a function of the temperature within the three-phase field  $\gamma + \alpha + \text{Gr}$  of the Fe-C equilibrium diagram. This field is sometimes referred to as the intercritical temperature interval (ITI). The limits of this three-phase field are defined by the chemical composition of the melt, mainly by its silicon content. The austenitizing stage is followed by an austempering step in order to produce the austenite-ausferrite reaction. Therefore, the final microstructure is composed of free allotriomorphic ferrite and ausferrite.

On the other hand, Wade et al. [2] and Verdu et al. [3] obtained IADI microstructures by means of heat treatments based on quick and incomplete austenitization cycles at temperatures within the austenite-graphite field (above the upper critical temperature of the ITI). Using this procedure, the austenite nucleates mainly around graphite nodules, and then it transforms into ausferrite during the austempering step. The amounts of ferrite and ausferrite are controlled by the austenitizing time: the longer the time, the greater the amount of austenite and, therefore, the larger the amount of ausferrite in the final microstructure.

Basso et al. [4,5], Kilicli et al. [6,7] and Fernandino et al [8-10] obtained IADI applying a different methodology. It consists in subjecting a fully ferritic DI to an incomplete austenitization stage, at different temperatures within the ITI, followed by an austempering step in order to transform austenite into ausferrite. This heat treatment has allowed to obtain microstructures composed of different percentages of ausferrite and allotriomorphic ferrite (original matrix of the samples), depending on the intercritical austenitizing temperature. The amount of ferrite increases when the austenitization step is closer to the lower limit temperatures of the ITI ( $T_{\text{lower}}$ ). On the other hand, when using austenitizing temperatures close to the upper limit temperatures of the ITI ( $T_{\text{upper}}$ ), the amount of allotriomorphic ferrite diminishes and it is present as a dispersed microconstituent in an ausferritic matrix.

The feasibility of economizing IADI production by eliminating the expensive ferritizing annealing heat treatment, which was assumed to be necessary to control properly the microstructure, was also analyzed by the authors in previous contributions [11,12]. It was found that proper IADI microstructures could be obtained from as-cast samples of high silicon DI (with Si contents greater than 3%). Another alternative thermal cycle has been also proposed by the authors [13]. In this case, the DI sample is initially austenitized within the austenite-graphite temperature field, to be then held at a temperature within the ITI in order to obtain the desired amount of ferrite. The main difference of this thermal cycle with respect to the prior ones is that the ferrite must now nucleate and grow into an austenitic matrix. The influence exerted by the chemical composition on the characteristics of the austenite-ferrite reaction occurring within the ITI of the Fe-C-Si diagram was also evaluated. The results showed a strong dependence between the alloy composition and the characteristics of the austenite-ferrite reaction, affecting the amount as well as the morphology of the precipitated allotriomorphic ferrite, which in some cases showed an intergranular morphology. The influence of the morphology and amounts of ferrite obtained by this last variant of heat treatment cycle on the mechanical properties of IADI has not been thoroughly investigated. This study is focuses on the analysis of the nucleation and growth of ferrite upon cooling previously austenitized DI samples into the ITI and below, in an attempt to identify the heat treatment conditions that lead to the precipitation of small amounts of intergranular ferrite. Then, the influence of each microstructure on the mechanical properties is evaluated.

## MATERIALS AND METHODS

### *Material and microstructural characterization*

**A**ll samples used in this work were obtained from a ductile iron melt alloyed with Cu and Mn to provide some degree of austemperability, necessary to obtain the same IADI microstructure throughout the whole volume of the samples [8]. The melt was prepared in a 50 kg capacity medium frequency induction furnace. Nodularization was carried out by using the sandwich method employing Fe–Si–Mg (6%). The melt was inoculated with Fe–Si (75%Si) and then, it was poured into 25 mm thick Y-block molds, which were prepared with alkyd resin bonded sand. The chemical composition was determined by using a Baird DV6 spectrometer. Metallographic samples were prepared by using standard polishing and etching methods. Etching was carried out by using nital (2%). The microconstituents were quantified by using an optical microscope and the Image Pro Plus software. The reported values from as-cast characterization are the average of at least three determinations. The graphite areas were not accounted for in the reported percentage of the microconstituents.

### *Determination of the upper and lower limit temperatures of the ITI*

The  $T_{\text{upper}}$  and  $T_{\text{lower}}$  temperatures were estimated using the methodology proposed by Gerval and Lacaze [14] and then, the advance of the transformation of ferrite into austenite as a function of the intercritical temperature was experimentally determined by heating prismatic small samples (10x10x60 mm) and held for 60 minutes at temperatures between 760°C and

900°C. After the holding stages were completed, the samples were water quenched. Then, the samples were sectioned and observed metallographically in order to quantify the amounts of ferrite and martensite present in the microstructure. This information is needed to properly design the heat treatment cycles aimed at obtaining IADI.  $T_{upper}$  and  $T_{lower}$  were experimentally determined as those temperatures that lead to a fully martensitic matrix, and that with 5% of martensite, respectively. It is worthy to note that these heat treatment cycles were performed on samples that were initially ferritized following an annealing heat treatment cycle consisting of an austenitizing stage at 920°C for 60 minutes followed by a slow cooling down to room temperature inside the furnace. This microstructural condition is commonly used to standardize the starting microstructure of the samples to be heat treated to determine the ITI [4-5,8-10].

#### *Study of kinetics of ferrite precipitation from austenite within the ITI*

Based on the values of  $T_{upper}$  and  $T_{lower}$  measured, heat treatments aimed at investigating the advance of the precipitation of ferrite from austenite were carried out as follows. Several sets of small samples were heated to full austenitizing temperature [910 °C] and maintained for 60 minutes. Then, the temperature of the furnace was reset to a temperature below  $T_{upper}$ . After different holding periods, samples were extracted and quenched in water. The thermal cycle is shown schematically on Fig. 1. After heat treatment, the samples were sectioned and observed metallographically in order to quantify the phases present at the microstructure.

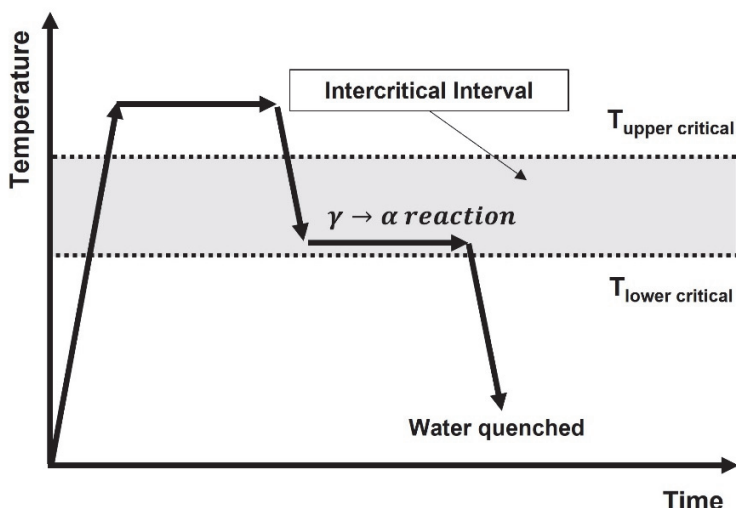


Figure 1: Thermal cycle used to investigate the precipitation of ferrite at temperatures within the ferrite-austenite-graphite temperature field.

#### *Heat treatments to obtain different LADI microstructures*

Based on the knowledge of the kinetics of ferrite precipitation, heat treatments intended to produce ferritic-ausferritic matrices were carried out as follows. Sets of tensile, impact and fracture toughness samples were heated and held for 60 minutes at full austenitizing temperature (910°C). Then, the temperature was decreased inside the furnace to reach a temperature within the ITI. The holding time at the intercritical temperature aimed at producing the precipitation of 5% to 15 % of free ferrite, since it was reported that these amounts of free ferrite led to interesting combinations of strength and elongation [15]. Then, the samples were austempered in a molten salt bath and held at two different temperatures. In this work, austempering steps were performed at 280 °C and 230 °C, for 90 minutes. Fully ausferritic (conventional ADI) samples austenitized at 910°C for one hour and then austempered at the same temperatures as those of the IADI samples, were also produced in order to evaluate the influence of free ferrite on high-strength ADI structures.

#### *Mechanical tests*

Rockwell hardness measurements were performed with a universal hardness testing machine Ibertest-DU 250 following the recommendations of ASTM E18. Tensile tests were carried out on small-size cylindrical specimens proportional to standard (0.25 in diameter.) following the recommendations of the ASTM E8M standard. A universal testing machine with a crosshead displacement rate of  $8.4 \times 10^{-3}$  mm s<sup>-1</sup> was used. Un-notched Charpy samples of 10x10x55 mm were tested following the ASTM E23 standard, using an impact machine that delivers an impact speed of 5 m s<sup>-1</sup>. Results were expressed



as impact energy measured in J\*cm<sup>-2</sup>. SEN(B) standard specimens of 10x20x100mm were used to determine the fracture toughness parameter KIC, following the specifications given by the ASTM E399 standard. The test specimens were pre-machined, heat treated and machined to final dimensions. For the case of impact and toughness samples, the notches were machined with conventional procedures and the pre-cracking was carried out in a fatigue machine with a double eccentric system, when needed. The final crack length was measured using a profile projector. All reported values of mechanical properties are the average of at least three tests.

## RESULTS

### *Chemical composition and as-cast characterization*

The chemical composition of the melt listed in Table 1. The as-cast microstructure is shown in Fig. 2. The result of as-cast characterization shows a metallic matrix composed of 90% perlite - 10% ferrite, a graphite nodularity of 90%, with a nodular count of about 120 [nod\*mm<sup>-2</sup>] according to ASTM A-247 standard.

Melt	Content (wt-%)						
	C	Si	Mn	Cu	S	P	C.E.
	3.47	2.99	0.41	0.38	0.020	0.024	4.46

Table 1: Chemical composition of the melt (Bal. Fe).

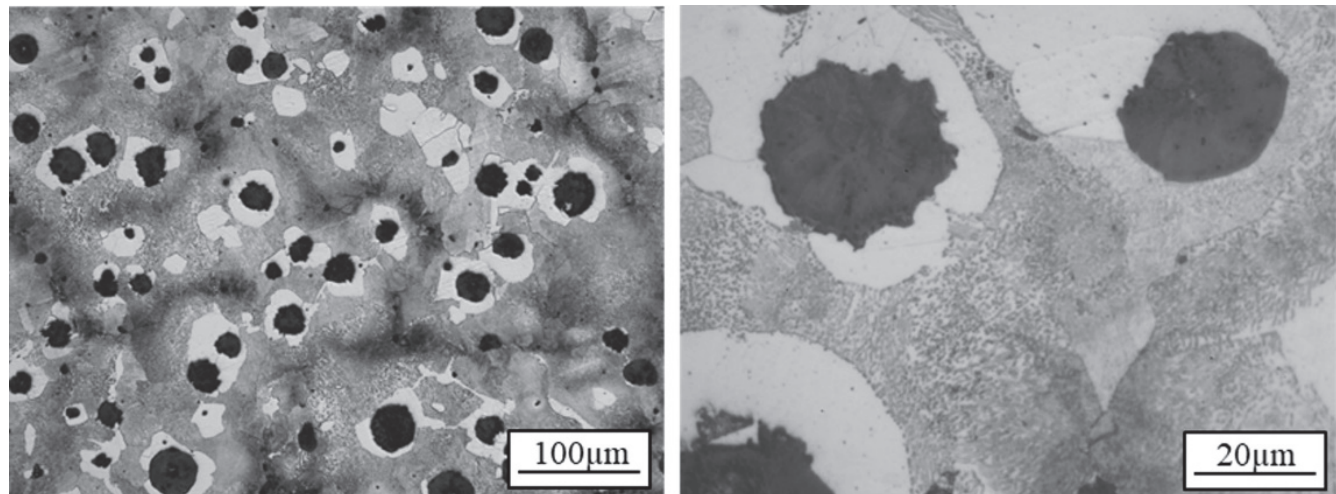


Figure 2: Optical metallography of the as-cast microstructure at different magnification. Nital 2%.

### *Intercritical temperature interval*

The microstructure of the samples resulting from the heat treatment cycles used for determining the  $T_{upper}$  and  $T_{lower}$  is shown in Fig. 3. The results of the phase quantification are plotted in Fig. 4. It is worth remembering that these samples were previously ferritized. According to the adopted criteria described early, the limit temperatures of the intercritical range for this alloy were determined as  $T_{upper}=860$  °C and  $T_{lower}=790$  °C. The values of  $T_{upper}$  and  $T_{lower}$  calculated by using the equations proposed by Gerval and Lacaze [14] resulted in  $T_{lower}=788$  °C and  $T_{upper}=823$  °C. The values of  $T_{lower}$  measured and calculated are in good agreement. The value of  $T_{upper}$ , on the other hand, is quite different, being the experimental reading much higher. This large difference may be a consequence of the microsegregation of the alloying elements, that causes a heterogeneous distribution of alloys elements at the metallic matrix. Additionally, it is important to mention that these values are the equilibrium phase percentages for each temperature, since according to previous work [4-6], a holding time of about 30 minutes is enough to reach the phase's equilibrium in the ferrite-austenite transformation within the ITI.

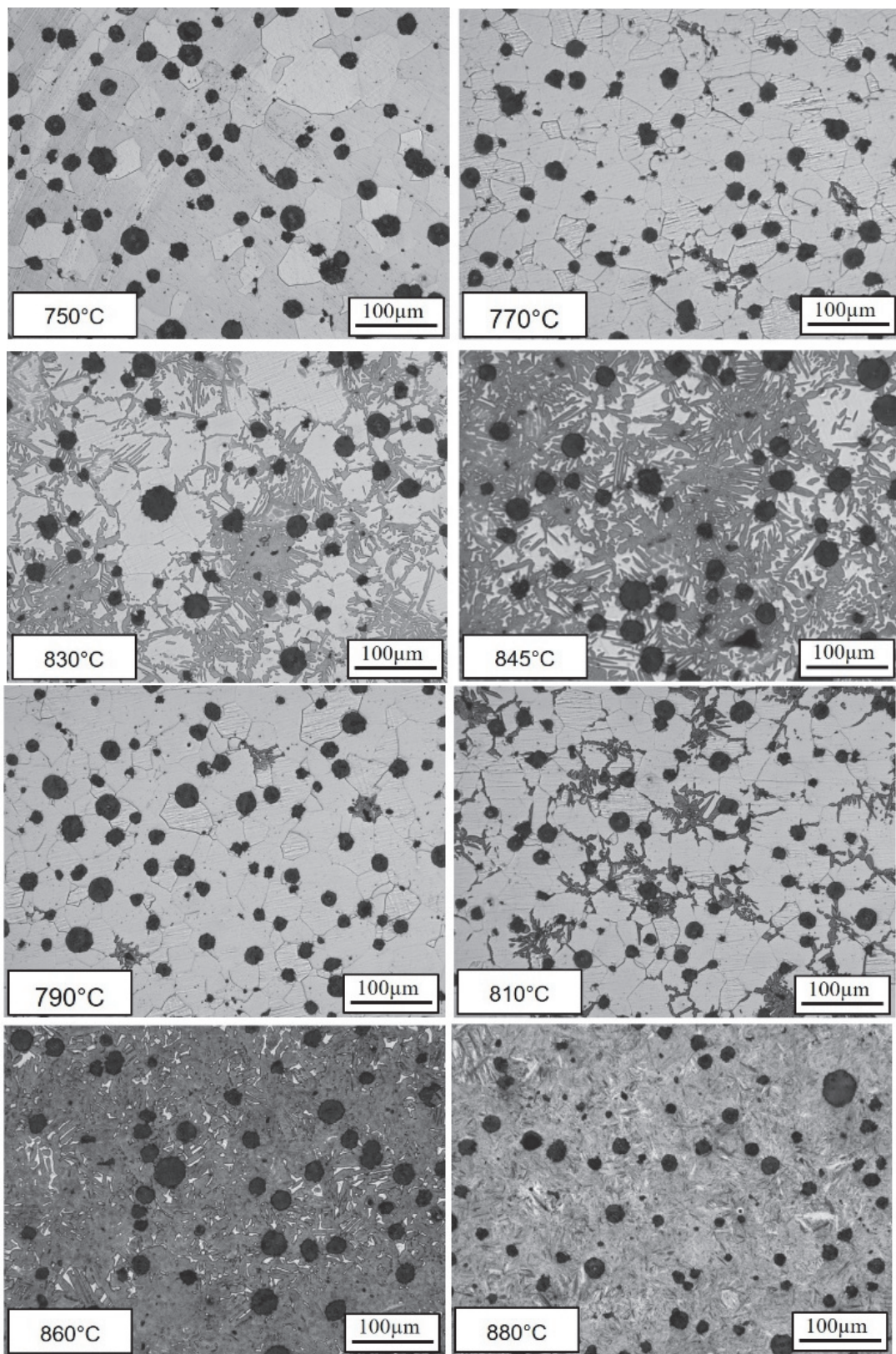


Figure 3: Metallographic samples resulting after heating ferritized samples at different temperatures within ITI and followed by quenching.

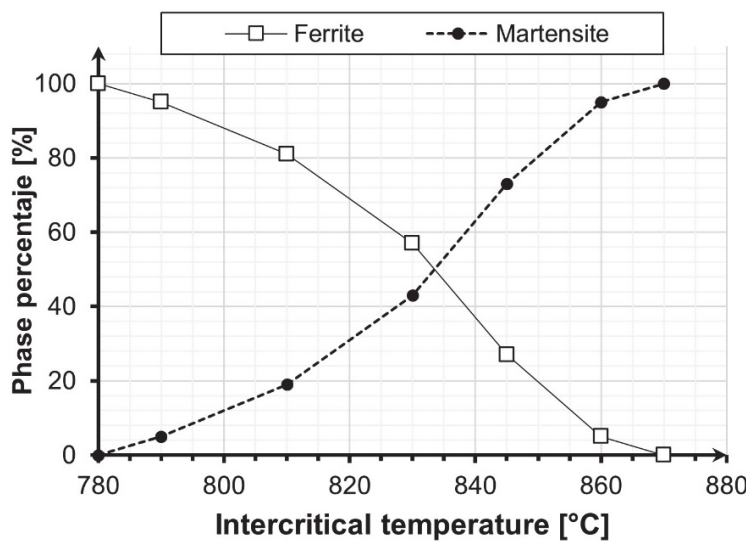


Figure 4: Phases quantification after quenching of samples heating at different temperatures.

#### *Study of kinetics of ferrite precipitation from austenite within the ITI*

Based on the results of  $T_{lower}$  and  $T_{upper}$ , isothermal cycles for intercritical austenitizing temperatures between 790°C and 840°C, after full austenitization at 910°C, were carried out for times ranging from 0 to 360 minutes, followed by quenching. Time 0 corresponds to the moment at which the samples, that are being cooled down inside the furnace from the fully austenitizing temperature, reach the preset temperature below  $T_{upper}$ . Fig. 5 shows the advance of ferrite precipitation for different intercritical temperatures and times. The reported values correspond to the amount of ferrite nucleated and grown from a fully austenitic matrix. For the intercritical temperatures of 790°C and 800°C, the reaction starts after approximately 30 minutes. For intercritical temperature of 810°C, transformation takes about 60 minutes to start, and it exceeds 120 minutes for an intercritical temperature of 840°C. It is clear that the rate of ferrite precipitation is strongly dependent of the intercritical austenitizing temperature. The greater the undercooling with respect to  $T_{upper}$ , the larger the driving force. However, even after 360 minutes of isothermal holding, the samples did not reach the amount of ferrite corresponding to the equilibrium at that temperature inside the ITI (see Fig. 4). For example, according to the equilibrium at 800°C, the amount of ferrite is approximately 85%, but under this heat treatment condition, the amount of ferrite obtained was just about 25% after 360 minutes. This noticeable difference evidenced in the characteristics of the austenite-ferrite reaction within the intercritical interval agree with the results reported by Basso et al [13], where the influence of chemical composition and holding time on austenite-ferrite transformation was analyzed.

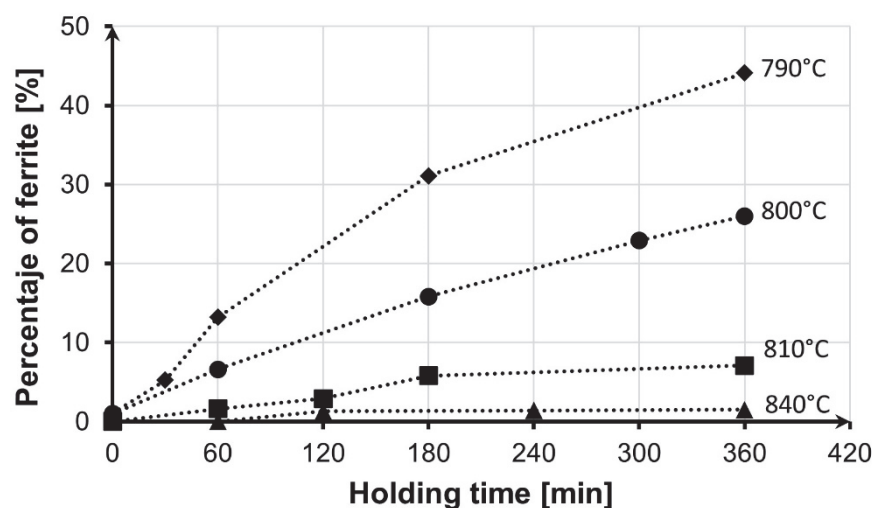


Figure 5: Percentage of ferrite as a function of intercritical austenitizing holding time.

Fig. 6 shows the microstructural evolution during the precipitation of ferrite with time for a holding temperature of 800°C. Ferrite precipitates are mostly concentrated along the austenite grain boundaries, and on the austenite graphite interface, as expected. It must be noted that graphite nodules only become enveloped by ferrite after a noticeable amount of ferrite has precipitated. In addition, the information about the ferrite precipitation kinetics should not be used to plot a conventional isothermal transformation diagram, as the cooling from the austenitizing temperature is not fast, nor is it controlled. Nevertheless, it quantifies well the amounts of ferrite that can be obtained in an actual heat treatment with similar parameters as those used here.

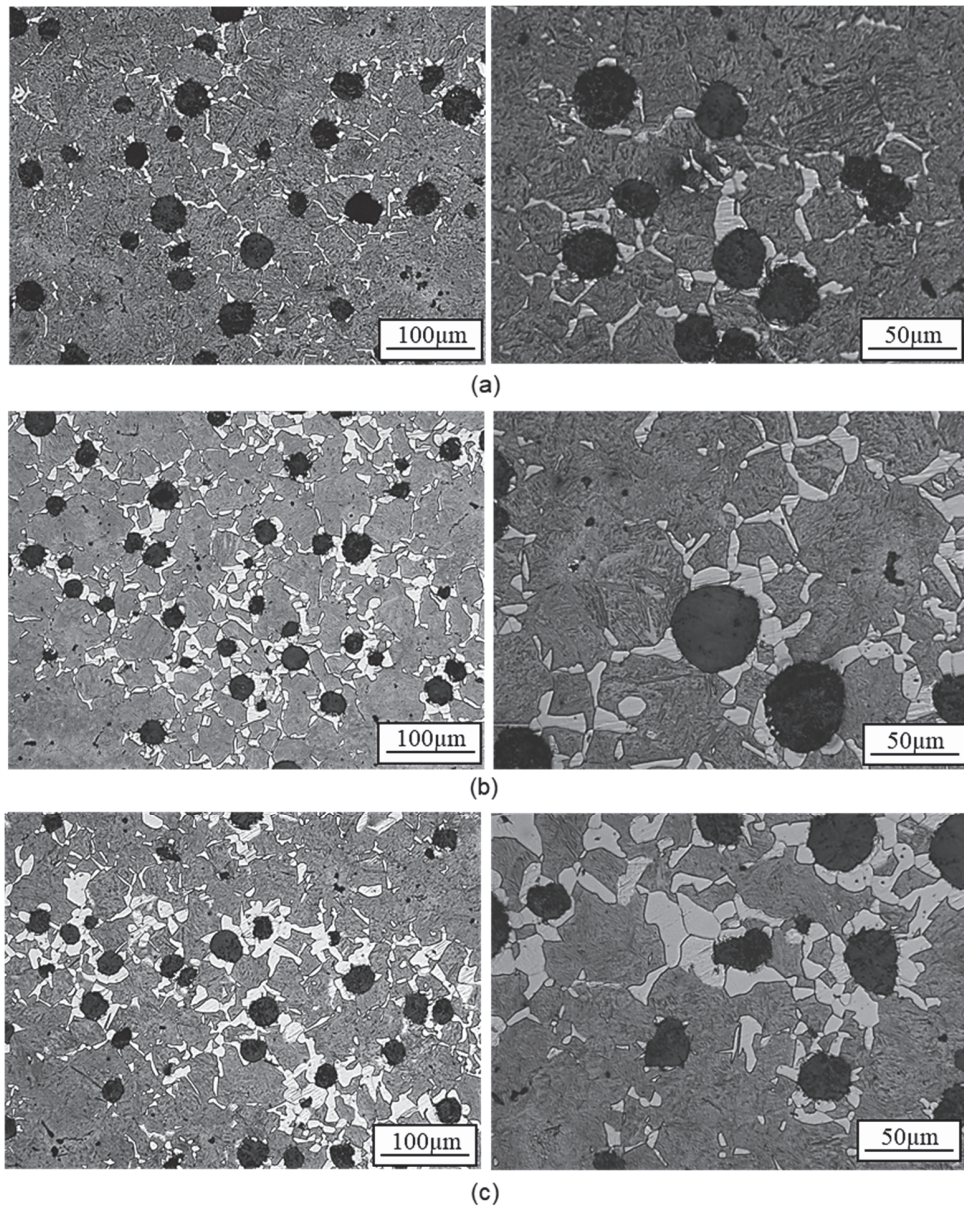


Figure 6: Advance of ferrite precipitation with time for 800°C holding temperature. (a) 60 min, (b) 120 min, (c) 360 min. Grey background is martensite and white is ferrite. Nital 2%.

#### *Heat treatments to obtain different high-strength LADI microstructures*

Based on the results of Fig. 6, heat treatments were conducted in order to evaluate the mechanical properties on the more interesting IADI microstructures. Testing samples were subjected to a fully austenitizing temperature of 910°C for 60 minutes, and then, samples were cooled to an intercritical austenitizing temperature of 800°C for two different holding times: 60 and 120 minutes, in order to obtain microstructures showing 5% and 15% of free ferrite, respectively. Later, the



austempering stage was carried out at 280°C and 230°C for 90 minutes. In this way, four different variants of high-strength IADI were evaluated: two microstructures composed of different amounts of ferrite and ausferrite, and two different austempering temperatures. Furthermore, for the two austempering temperatures, fully austempered samples (high-strength ADI grades) were also obtained and tested as a reference material. The different microstructures were named as follows: IADIT $\gamma$ -t and ADIT $\gamma$ , where t is the holding time and T $\gamma$  is the austempering temperature.

As example, ADI and IADI microstructures obtained after austempering at 280°C are shown in Fig. 7. The amount of free ferrite obtained were 5% and 15% after 60 and 120 minutes respectively, which are in good agreement with the previous quenching experiments.

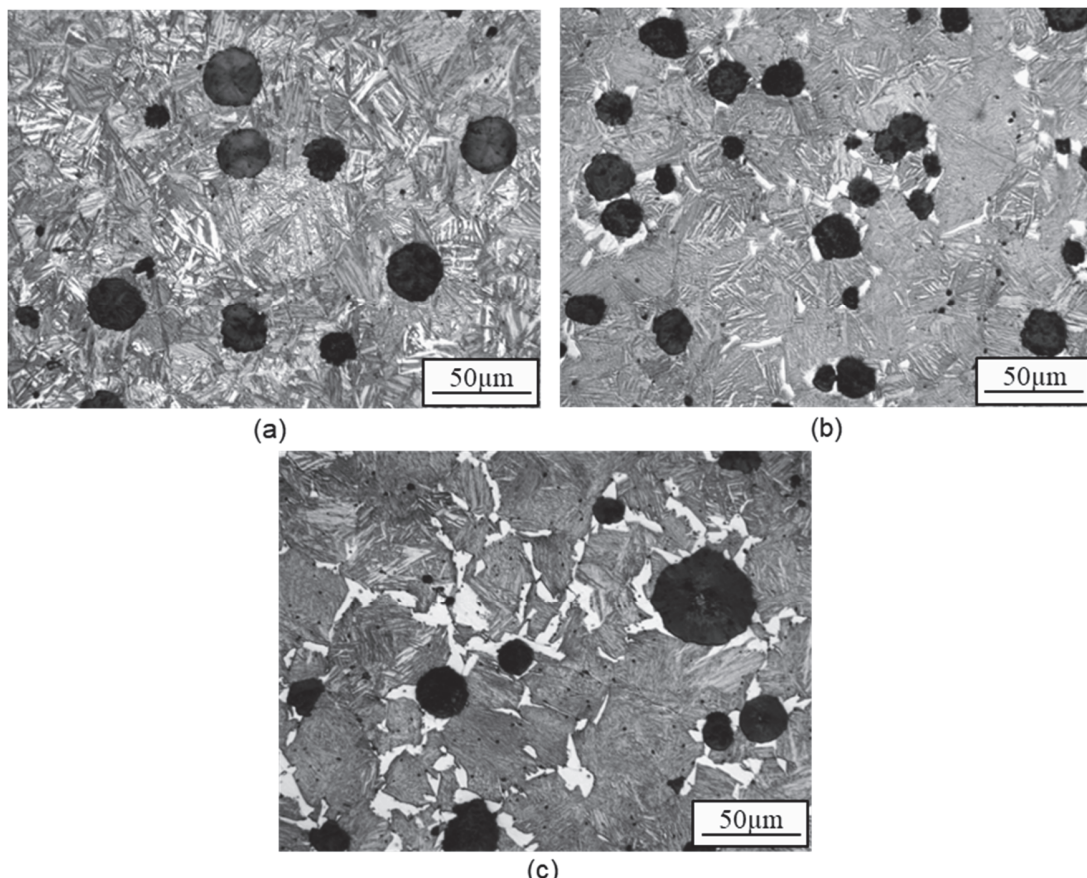


Figure 7: ADI and IADI microstructures obtained after austempering at 280 °C. (a) ADI280, (b) IADI280-60, (c) IADI280-120. Grey background is ausferrite and white is ferrite. Nital 2%.

### *Mechanical properties*

The values of hardness, ultimate tensile strength (UTS), yield stress and elongation until failure (%) measured on the ADI and IADI samples are plotted in Fig. 8. The results for ADI satisfy the requirements of Standard ASTM A857 Grade 1600-1300-01 for ADI 230, and Grade 1400-1100-02 for ADI 280. This shows that the quality of the base DI and the heat treatment used is suitable to produce standard ADI quality. The results of tensile tests of the IADI samples show that the presence of small amounts of free ferrite has some influence on the mechanical properties. For IADI microstructures austempered at 280°C (Fig. 8a), as the matrix includes a 5% and 15% of free ferrite, the yield strength and UTS decrease very little (1.5 and 3% respectively), while the elongation increases by about 50%. Nevertheless, it must be noted that the large relative increment in elongation consists only in an increase of the value of deformation to rupture from 2% to 3%. All these changes indicate a moderate but consistent increase in ductility with little decrease in strength. For samples austempered at 230°C, the drop in strength parameters is more marked, with a decrease ranging from 11% to 14% as the amount of ferrite grew from 5% to 15%. These changes were accompanied by gains in elongation from 33 to 100% (Fig. 8b).

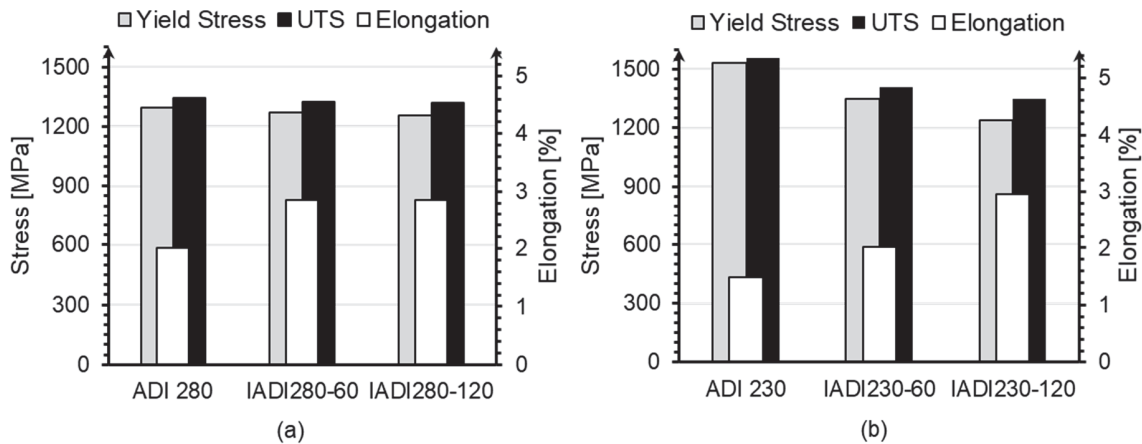


Figure 8: Results of tensile strength (UTS), yield stress and elongation (%) for ADI and IADI microstructures.

Regarding hardness, Tab. 2 shows a decrease as the holding time increases, for both austempering temperatures investigated. For all measurements, the experimental dispersion was about 5%. For samples austempered at 280°C, the hardness drops 10% and 18% when the amount of free ferrite presents in the microstructure changes from 5% to 15% respectively. For IADI's austempered at 230 °C, the hardness dropped from 5% to 8%.

Samples	Hardness [HRC]
ADI <sub>280</sub>	47
IADI <sub>280-60</sub>	43
IADI <sub>280-120</sub>	39
ADI <sub>230</sub>	51
IADI <sub>230-60</sub>	49
IADI <sub>230-120</sub>	47

Table 2: Results of hardness for ADI and IADI microstructures.

Fig. 9 shows the KIC values for the ADI and IADI samples. The highest KIC values are obtained for ADI280 microstructure (~ 76 MPa\*m<sup>0.5</sup>), and then, for the IADI280 variants. It is evident that as the amount of ferrite in the microstructure increases, the KIC value decreases. The presence of 15% of free ferrite produces a reduction of approximately 25% in the KIC value with respect to the ADI280. This is because the ferrite has lower toughness than the ausferrite obtained at 280 °C. The literature reports that the KIC of ferritic DI is about 50 MPa m<sup>0.5</sup> [5]. For the case of samples austempered at 230 °C, the KIC values do not change with the increase of ferrite in the microstructure. The ADI and IADI microstructures austempered at 230 °C show a KIC value of approximately 51 MPa m<sup>0.5</sup>. For this case, the KIC values of ADI230, and a ferritic DI are similar, then there are no changes in the fracture toughness of the material when the relative amounts of those phases vary in the microstructure. The explanation of the influence of the dispersion of ferrite on ausferrite based on the individual contribution of each micro-constituents appears, at a first sight, an oversimplification of the matter. In fact, in previous work [5], it was found that a small amount of free ferrite (~ 5%) present as a second dispersed phase in IADI austempered at 350°C, improved the KIC value in comparison with fully ausferritic matrix by 14%. This result was attributed to events taking place ahead of the advancing crack front [17]. Fracture toughness is enhanced through the deflection of the crack path as it advances through the material. Then, it is possible to assume that the presence of the dispersed ferrite could serve to shield the crack tip, increasing fracture toughness levels. Nevertheless, the results of our investigation do not support this hypothesis. Indeed, the decrease of the fracture toughness as ferrite is dispersed in the matrix could be attributed to the ferrite morphology in the IADI microstructures. The presence of ferrite as a second phase of a high degree of continuity could generate a preferential path for the propagation of cracks, generating a decrease in fracture toughness with respect to the completely ausferritic microstructures (ADI). New studies are currently under way in order to confirm this mechanism.

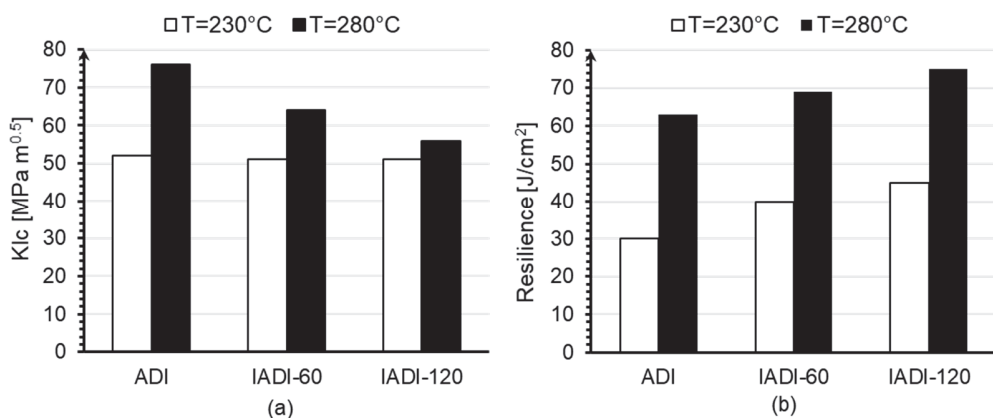


Figure 9: Results of impact test and fracto-mechanical properties ( $K_{IC}$ ) for ADI and IADI microstructures.

Regarding impact properties, Fig. 9 shows the resilience values for ADI and IADI samples. For both austempering temperatures under study, the presence of free ferrite improves de impact properties of ADI and IADI microstructures. The impact energy increases for about 10 % and 20% for IADI's containing 5% and 15% of free ferrite in the microstructure, in comparison with ADI280. It is important to highlight the increment of the impact energy for samples austempered at 230°C. The resilience increases about 33% and 50% for IADI's containing 5% and 15% of free ferrite in the microstructure, with respect to ADI230. It is clear that this small amount of ferrite (ductile phase) present in the microstructure promotes an improvement in the impact properties of ADI.

In summary, the changes in mechanical and fracture properties were modest but positive for the potential structural application of IADI. An important improvement in impact properties was produced by adding small amounts of free ferrite on high strength grades ADI. Further research should be conducted to quantify the improvement that can be reached in higher strength grades of austempered irons.

## CONCLUSIONS

The following conclusions can be highlighted:

- A new heat treatment procedure was developed and applied to produce Intercritical Austempered Ductile Irons (IADI). The heat treatment involves a full austenitization of the metallic matrix followed by an intercritical annealing step within the intercritical interval, and a final austempering stage.
- The use of this heat treatment led to a microstructure composed by different amounts of ausferrite and dispersed free ferrite. It makes it possible to produce microstructures consisting in ausferritic matrices containing continuous and well-defined networks of allotriomorphic ferrite, located at the grain boundaries of the recrystallized austenite.
- Tensile properties were evaluated in IADI microstructures containing 5 and 15% of free ferrite in their microstructure, and austempered at 230 °C and 280 °C. When compared to fully austempered samples, it was found that as the amount of free ferrite increases, tensile strength and yield stress diminishes, while elongation increase, for all the austempering temperatures evaluated.
- The addition of free ferrite on ADI microstructures improved the impact toughness but not the fracture toughness.
- The best combinations of mechanical properties for mixed structures were obtained by using the higher austempering temperature evaluated (280 °C in the present study).

## ACKNOWLEDGEMENTS

This work has been supported by grants awarded by ANPCyT and MINCyT of Argentina and Fondo para la Investigación Científica y Tecnológica [grant number PICT 12-1146 and PICT 14-3038].



## REFERENCES

- [1] Aranzábal, J., Serramoglia, G. and Rousiere, D. (2002). Development of a new mixed (ferritic – ausferritic) ductile iron for automotive suspension parts. *Int. J. Cast Met.* 16, pp. 185-190. DOI:10.1080/13640461.2003.11819580.
- [2] Wade, N. and Ueda, Y. (1981). Mechanical Properties of Ductile Cast Iron with Duplex Matrix. *Transactions ISIJ* 21 (2), pp. 117-126. DOI:10.2355/isijinternational1966.21.119.
- [3] Verdu, C., Adrien, J. and Reynaud, A. (2005). Contributions of dual phase heat treatments to fatigue properties of SG cast irons. *Int. J. Cast Met. Res.* 18, pp. 346-354.
- [4] Basso, A., Martínez, R. and Sikora, J. (2006). Development of Dual Phase ADI. Proc. Eighth International Symposium on Science and Processing of Cast Iron, Beijing, China, pp. 408-413.
- [5] Basso, A., Martínez, R. and Sikora, J. (2007). Influence of austenitising and austempering temperatures on microstructure and properties of dual phase ADI. *Mater. Sci. Technology*. 23, pp. 1321-1326. DOI:10.1179/174328407X236544.
- [6] Kilicli, V. and Erdogan, M. (2006). Tensile properties of partially austenitised and austempered ductile irons with dual matrix structures. *Mater. Sci. Technology*. 22, pp. 919-928. DOI:10.1179/174328406X102390.
- [7] Kilicli, V. and Erdogan, M. (2007). Effect of ausferrite volume fraction and morphology on tensile properties of partially austenitised and austempered ductile irons with dual matrix structures. *Int. J. Cast Met.* 20, pp. 202-214. DOI:10.1179/136404607X256051.
- [8] Fernandino, D.O., Massone, J.M. and Boeri, R.E. (2013). Characterization of the austemperability of partially austenitized ductile iron. *Journal of Materials Processing Technology* 213, pp. 1801-1809. DOI:10.1016/j.jmatprotec.2013.05.002.
- [9] Fernandino, D.O., Boeri, R., Di Cocco, V., Bellini, C. and Iacoviello, F. (2020). Damage evolution during tensile test of austempered ductile iron partially austenized. *Mat Design Process Comm.* e157. DOI:10.1002/mdp.2157
- [10] Fernandino, D.O., Di Cocco, V., Iacoviello, F. and Boeri, R. (2020). Microstructural damage evaluation of ferritic-ausferritic Spheroidal Graphite Cast Iron. *Frattura ed Integrità Strutturale* 51, pp. 477-485. DOI:10.3221/IGF-ESIS.51.36.
- [11] Basso, A., Caldera, M. and Massone, J. (2015). Development of high silicon Dual Phase ADI. *ISIJ Int.* 55, pp. 1106–1113. DOI:10.2355/isijinternational.55.1106.
- [12] N.E. Tenaglia, D.I. Pedro, R.E. Boeri, A.D. Basso. (2020). Influence of silicon content on mechanical properties of IADI obtained from as cast microstructures. *Int. J. Cast Met Res.* 33(2-3), pp. 72-79. DOI:10.1080/13640461.2020.1756082
- [13] Basso, A., Martínez, R.A. and Sikora, J.A. (2011). Influence of chemical composition and holding time on austenite ( $\gamma$ ) → ferrite ( $\alpha$ ) transformation in ductile iron occurring within the intercritical interval. *Journal of Alloys and Compounds*, 509, pp. 9884-9889. DOI:10.1016/j.jallcom.2011.07.069.
- [14] Gerval, V. and Lacaze, J. (2000). Critical temperature range in spheroidal graphite cast irons, *ISIJ International* 40 (4), pp. 386-392. DOI:10.2355/isijinternational.40.386.
- [15] Basso, A., Sikora, J.A. and Martínez, R.A. (2013). Analysis of mechanical properties and its associated fracture surfaces in dual-phase austempered ductile iron. *Fatigue Fract Engng Mater Struct.* 36, pp. 650–659. DOI:10.1111/ffe.12032.
- [16] Smithells, C.J. (1992). Metals reference book. 7th edition. Edited by E.A.Brandes & G.B.Brook. Butterworth Heinemann. Chapter 13: Diffusion in metals. DOI:10.1016/B978-0-08-051730-8.50018-2.
- [17] Hertzberg, R.W. (1996) Deformation and Fracture Mechanics of Engineering Materials. 4th Edition, John Wiley & Sons, Inc., Hoboken.

## NOMENCLATURE

DI: Ductile Iron

ADI: Austempered Ductile Iron

IADI: Intercritically Austempered Ductile Iron

ITI: Intercritical Temperature Interval

$T_{lower}$ : Lower limit temperatures of the ITI

$T_{upper}$ : Upper limit temperatures of the ITI